Immune-based biomarker accurately predicts response to imiquimod immunotherapy in cervical high-grade squamous intraepithelial lesions

Abdulrahman, Z.; Hendriks, N.; Kruse, A.J.; Somarakis, A.; Sande, A.J.M. van de; Beekhuizen, H.J. van; ... ; Esch, E.M.G. van

Journal for ImmunoTherapy of Cancer

Immune-based biomarker accurately predicts response to imiquimod immunotherapy in cervical high-grade squamous intraepithelial lesions

Ziena Abdulrahman ,[1,2] Natasja Hendriks,[3] Arnold J Kruse,[3] Antonios Somarakis,[1] Anna J M van de Sande,[4] Heleen J van Beekhuizen,[4] Jurgen M J Piek,[5] Noel F C C de Miranda ,[1] Loes F S Kooreman,[3] Brigitte F M Slangen,[3] Sjoerd H van der Burg ,[1,2] Peggy J de Vos van Steenwijk,[3] Edith M G van Esch[5]

To cite: Abdulrahman Z, Hendriks N, J Kruse A, *et al*. Immune-based biomarker accurately predicts response to imiquimod immunotherapy in cervical high-grade squamous intraepithelial lesions. *Journal for ImmunoTherapy of Cancer* 2022;**10**:e005288. doi:10.1136/jitc-2022-005288

► Additional supplemental material is published online only. To view, please visit the journal online (http://dx.doi.org/10.1136/jitc-2022-005288).

SHvdB, PJdVvS and EMGvE contributed equally.

Accepted 13 September 2022

[1]Leiden University Medical Center, Leiden, The Netherlands
[2]Oncode Institute, Utrecht, The Netherlands
[3]Maastricht University Medical Centre+, Maastricht, The Netherlands
[4]Erasmus Medical Center, Rotterdam, The Netherlands
[5]Catharina Hospital, Eindhoven, The Netherlands

Correspondence to
Dr Edith M G van Esch; edith.v.esch@catharinaziekenhuis.nl

ABSTRACT

Background The complete response rate of cervical high-grade squamous intraepithelial lesion (cHSIL) patients to imiquimod immunotherapy is approximately 60%. Consequently, many patients are exposed to unnecessary adverse effects of imiquimod. On the other hand, conventional surgical large loop excision therapy is associated with increased risk of premature births in subsequent pregnancies. An in-depth analysis of the cHSIL immune microenvironment was performed in order to identify and develop a predictive biomarker for response to imiquimod, to maximize therapy efficacy and to avoid adverse effects in patients unlikely to respond.

Methods Biopsies of 35 cHSIL patients, before and 10 weeks on imiquimod treatment, were analyzed by two multispectral seven-color immunofluorescence panels for T cell and myeloid cell composition in relation to treatment response. Based on these results a simplified immunohistochemical detection protocol was developed. Samples were scanned with the Vectra multispectral imaging system and cells were automatically identified using machine learning.

Results The immune microenvironment of complete responders (CR) is characterized by a strong and coordinated infiltration by T helper cells (activated PD1$^+$/type 1 Tbet$^+$), M1-like macrophages (CD68$^+$CD163$^-$) and dendritic cells (CD11c$^+$) prior to imiquimod. The lesions of non-responders (NRs) displayed a high infiltration by CD3$^+$FOXP3$^+$ regulatory T cells. At 10 weeks on imiquimod, a strong influx of intraepithelial and stromal CD4$^+$ T cells was observed in CR but not NR patients. A steep decrease in macrophages occurred both in CR and NR patients, leveling the pre-existing differences in myeloid cell composition between the two groups. Based on the pre-existing immune composition differences, the sum of intraepithelial CD4 T cell, macrophage and dendritic cell counts was used to develop a quantitative simplified one color immunohistochemical biomarker, the CHSIL immune biomarker for imiquimod (CIBI), which can be automatically and unbiasedly quantified and has an excellent predictive capacity (receiver operating characteristic area under the curve 0.95, p<0.0001).

Conclusion The capacity of cHSIL patients to respond to imiquimod is associated with a pre-existing coordinated local immune process, fostering an imiquimod-mediated increase in local T cell infiltration. The CIBI immunohistochemical biomarker has strong potential to select cHSIL patients with a high likelihood to experience a complete response to imiquimod immunotherapy.

WHAT IS ALREADY KNOWN ON THIS TOPIC

⇒ Cervical high-grade squamous intraepithelial lesion (cHSIL) is conventionally treated by surgical large-loop excision, which increases the chance of premature births in following pregnancies, therefore, imiquimod immunotherapy is explored, 60% of patients respond to imiquimod.

WHAT THIS STUDY ADDS

⇒ Here, we developed a new immune-based immunohistochemical biomarker that accurately predicts response to imiquimod, which can be applied on routinely taken pretherapy biopsies, the cHSIL immune biomarker for imiquimod (CIBI).

HOW THIS STUDY MIGHT AFFECT RESEARCH, PRACTICE OR POLICY

⇒ CIBI will enable personalized therapy for cHSIL patients, thereby minimizing side effects and maximizing therapy adherence.

INTRODUCTION

Cervical high-grade squamous intraepithelial lesion (cHSIL), also referred to as cervical intraepithelial neoplasia (CIN) 2 and 3, is a premalignant lesion induced by a persistent infection with high-risk human papillomavirus (hrHPV). The incidence of cHSIL is rising worldwide, especially among young women.[1] Conventionally cHSIL is treated by large loop excision of the transformation

zone (LLETZ), with potential complications such as hemorrhage, infection and an increased risk of premature birth in subsequent pregnancies. Furthermore, surgical treatment strategies are ineffective in 10% of patients, resulting often in difficult to treat recurrences, repeated treatments or even hysterectomy.[2]

The topical application of immunomodulating imiquimod cream (Aldara/Zyclara), a toll-like receptor 7 (TLR7) agonist, is a new treatment strategy for cHSIL. TLR7 is expressed by antigen presenting cells, such as macrophages and dendritic cells (DCs), and upon binding to imiquimod an intracellular inflammatory cascade is activated. This results in the secretion of proinflammatory cytokines such as IFNγ, TNFα and IL-12, the attraction and activation of other immune cells to the lesion, and the polarization of T cells to a type 1 oriented and cytotoxic T cell response, hereby amplifying the local immune response.[3] Previous clinical trials have shown that about 60% of cHSIL patients display a clinical response to topical imiquimod therapy.[4 5] Adverse effects of imiquimod therapy are common and can be extensive, consisting mostly of local inflammation and burning, but also of systemic adverse events (headache and influenza-like symptoms).[6] The adverse effects and long treatment duration of 16 weeks turns therapy adherence into a challenge with up to 20% discontinuation.[7] Predictive biomarkers to prevent overtreatment and to increase therapy efficacy and adherence are highly warranted.

We have previously shown that the immune microenvironment is of major importance for response to imiquimod in vulvar HSIL (vHSIL), which is also caused by a persistent hrHPV infection, but at a different anatomical site. In vHSIL, a pre-existing coordinated infiltration by $CD4^+$ and $CD8^+$ T cells as well as inflammatory $CD14^+$ myeloid cells is associated with complete response on imiquimod therapy.[8] To our knowledge, no studies have been published on the effects of imiquimod on the immune microenvironment in cHSIL, nor if the composition of the pre-existing immune microenvironment can be used as predictive biomarker. Therefore, we performed a comprehensive in-depth characterization of the immune microenvironment using multispectral immunofluorescence on a unique cohort of cHSIL patients treated with topical imiquimod, investigating both pretreatment and on-treatment cHSIL tissue, in the context of their clinical response. Here, we show that imiquimod has the strongest effect on immune cell composition in lesions with high pre-existing immunity. In addition, specifically a strong pre-existing infiltration by $CD3^+CD8^-FOXP3^-$ T cells, $CD68^+CD163^-$ M1-like macrophages and $CD11c^+$ DCs accurately distinguished complete responders (CRs) from non-responders (NRs). This observation allowed the development of a simple unbiased predictive and sensitive one color immunohistochemical biomarker for imiquimod response (receiver operating characteristic area under the curve (ROC AUC) 0.95, p<0.0001) that is easily applicable in routine diagnostics, the CHSIL immune biomarker for imiquimod (CIBI).

MATERIALS AND METHODS

Patient samples

Pretreatment and on imiquimod treatment formalin-fixed paraffin-embedded (FFPE) biopsies of 35 women with histologically confirmed cHSIL included in the TOPIC trial (NCT02917746) were analyzed. The TOPIC trial was performed at three hospitals in the Netherlands: Maastricht University Medical Center (which provided medical ethical approval for performing this study in the Netherlands, NL57849.068.16/METC162025), Erasmus University Medical Center Rotterdam and Catharina Hospital Eindhoven, where after providing written informed consent patients were treated with a 16-week imiquimod treatment regimen consisting of 6.25 mg (half a sachet) imiquimod 5% cream administered vaginally three times a week, instead of standard therapy by LLETZ. Biopsies were 3–5 mm diameter in size, and the entire cHSIL region in the biopsies was analyzed.[7] This study was conducted in accordance with the Declaration of Helsinki and in accordance with Dutch law. Biopsies were taken at three time points: pre-imiquimod (diagnostic), on imiquimod treatment (10 weeks) and after imiquimod treatment (20 weeks). The 20-week biopsies were not analyzed due to the small sample size (3 NR already had received LLETZ treatment due to lesion progression and 10 CR had complete lesion clearance at that time).

HPV genotyping was performed using PCR enzyme immunoassays on either cytological or histological samples. DNA isolation of the samples was performed with the Maxwell 16 kit (Promega). A PCR GP5+/6+was run with universal HPV primers, and HPV positivity was assessed with agarose gel electrophoresis. HPV positive samples were subsequently subtyped using an enzyme immunoassay for the detection of HPV16, HPV18, or cocktail hrHPV (31, 33, 35, 39, 45, 51, 52, 56, 58, 59, 66).

An NR was defined as having a persistent HSIL (HPV^+CIN2 and CIN3) at 20 weeks, which was an indication for LLETZ. Patients with no dysplasia, CIN1 or HPV^-CIN2 at 20 weeks underwent 6 months of follow-up conform standard care, and after 6 months a PAP smear for cytological assessment was taken. Complete response (CR) was defined as cytologically confirmed lesion clearance at 6 months (PAP1), and partial response (PR) was defined as >PAP1 at 6 months. An overview of the study workflow is presented in online supplemental figure 1.

Multispectral immunofluorescence staining

Two previously published seven-color multispectral immunofluorescence panels were applied, one for T cells, consisting of CD3, CD8, FOXP3, TIM3, Tbet, PD-1, DAPI, and one for myeloid cells, consisting of CD14, CD33, CD68, CD11c, CD163, PD-L1, DAPI.[8 9] In these panels, a combination of indirect detection (fluorochrome labeled secondary antibody) and direct detection (primary antibody directly labeled with fluorochrome, for antibodies with clashing species/isotypes) of markers was used. Dim markers (PD-L1, PD-1, and Tbet) were tyramide signal amplified with Opal (PerkinElmer)

to enable their detection by fluorescence microscopy. An overview of the antibodies and immunodetection methods included in each panel are shown in online supplemental table 1A,B. Optimal antigen retrieval buffers were determined for all individual markers by performing stainings in both citrate and tris-EDTA, the buffer in which all antibodies of a panel performed well was then chosen for that panel. In short, the slides were stained as follows: on the first day, 4 µm thick FFPE tissue sections were deparaffinized, endogenous peroxidase was blocked with 0.3% hydrogen peroxide and heat induced epitope retrieval was performed in the T cell panel with citrate (10 mM, pH 6.0) and in the myeloid cell panel with tris-EDTA (10 mM/1 mM, pH 9.0). SuperBlock (ThermoFisher Scientific) was used to block non-specific binding sites. First, the primary antibodies detected by Opal were applied and amplified according to the manufacturer's protocol. Then the unconjugated primary antibodies were incubated overnight at room temperature. On the second day, the corresponding fluorescently labeled secondary antibodies were applied, followed by 5 hours incubation with the directly labeled primary antibodies. Finally, DAPI was applied as nuclear counterstain and slides were mounted.[8]

Dual immunohistochemical staining

A new dual immunohistochemistry panel was designed, consisting of the markers CD4, CD68 and CD11c (all three rabbit IgG antibodies) stained with DAB (brown), and the markers FOXP3 and CD163 (both mouse IgG antibodies) stained with Vector Red (red), using the ImPRESS Duet double staining polymer kit (Vector laboratories). On the first day, 4 µm thick tissue sections were deparaffinized, endogenous peroxidase was blocked with 0.3% hydrogen peroxide, and heat induced epitope retrieval was performed with citrate (10 mM, pH 6.0). Non-specific binding sites were blocked with normal horse serum 2.5% for 20 min, and the mix of all five primary antibodies (CD4, CD68, CD11c, FOXP3, CD163, panel design included in online supplemental table 1C) was incubated overnight at 4°C. The following day slides were incubated with a mix of horseradish peroxidase (HRP) horse-anti-rabbit IgG and alkaline phosphatase (AP) horse-anti-mouse IgG for 10 min, and subsequently antibody binding was detected with DAB (oxidized by HRP to a brown chromogen, 5 min incubation) and Vector Red (oxidized by AP to a red chromogen, 30 min incubation). Nuclei were counterstained with hematoxylin and slides were dehydrated and mounted.

Quantification of immune cells in the tumor microenvironment

As published,[8] images of the entire tissue sections stained with the multispectral immunofluorescence or immunohistochemical panels were acquired with the Vectra 3.0.5 multispectral imaging microscope (PerkinElmer) at ×20 magnification. Immune cells in the tumor microenvironment (TME) of both the immunofluorescence and immunohistochemical images were automatically phenotyped and counted with inForm V.2.4 image analysis software (PerkinElmer-Akoya Biosciences) after manual training. The software was trained to segment epithelium and stroma, segment $DAPI^+$ or $hematoxylin^+$ nucleated cells, and assign a phenotype to each cell. All phenotypes were visually inspected on accurateness, and if errors were detected the training was further optimized until all discrepancies were resolved. Immune cell counts were normalized for tissue size (cells/mm^2 epithelium and cells/mm^2 stroma). Cell phenotypes above the threshold of a median cell count ≥10 cells/mm^2 in at least one response group and at least one time point were included in the analyses, in order to study biologically common cell phenotypes and not to focus on chance findings, as published before.[8]

Spatial cellular interaction analyses

Spatial high-dimensional cell-cell interaction analyses were performed using a new version of ImaCyte developed for spatial analyses on multispectral immunofluorescence images (in-house developed program, available from https://github.com/biovault/ImaCytE).[10 11] Similar to others,[12 13] permutation testing with 1000 iterations was applied to identify spatial interactions that occurred more frequently than expected based on chance, hereby correcting for differences in cell phenotype frequencies among response groups. Only interactions with a permutation based Z-score >2 (ie, outside the 95% normal distribution range, so unlikely to be spatially located next to each other by chance) were included for further analyses. To study differences in spatial interactions across two subgroups (NR vs CR), interactions with a permutation-based Z-score >2 (ie, spatial interaction) in one of the subgroups and a permutation-based Z-score<-2 (ie, spatial separation) in the other subgroup were included in the analyses (thus all opposite spatial interactions).

Statistical analyses

Statistical data analysis was performed with GraphPad Prism V.8.0.1 (GraphPad Software), which was also used to create graphs to visualize the data. The median immune counts of the two different response groups (NR vs CR) were compared with the non-parametric Mann-Whitney U test. PRs were not included in the statistical analyses due to their small sample size (n=3). Differences between pretreatment and on imiquimod treatment immune cell infiltration were compared with the non-parametric Wilcoxon paired signed rank test. Spearman correlation was used to study correlations between the T cell and myeloid cell infiltrate. Two-sided p values <0.05 were marked as statistically significant.

RESULTS

Imiquimod induces a strong intraepithelial influx by T cells and a decrease in macrophages

To investigate the impact of imiquimod on the immune microenvironment, we compared the lymphoid and myeloid immune cell composition of pre-imiquimod cHSIL biopsies (n=35) versus the on treatment biopsies (n=27, 8 samples were excluded; 6 CR because they had already regressed and only contained healthy cervical

tissue, 1 PR whose sample was missing, 1 NR with a sampling error that only contained healthy tissue). An overview of the patient characteristics is provided in table 1. To enable in-depth immune cell characterization, multispectral immunofluorescence was applied (figure 1A,B). Eleven different T cell phenotypes and twelve different myeloid cell phenotypes were identified in cHSIL. The major T cell populations were $CD3^+CD8^-FOXP3^-$ T helper cells, $CD3^+CD8^+FOXP3^-$ T cells and $CD3^+CD8^-FOXP3^+$ regulatory T cells, either activated ($TIM3^+/PD1^+$) or not, and with a type 1 cytokine profile ($Tbet^+$) or not. The major myeloid populations were $CD68^+CD163^-$ M1-like macrophages, $CD68^+CD163^+$ M2-like macrophages, $CD14^+CD68^-CD11c^-$ inflammatory monocytes, $CD14^-CD68^-CD11c^+$ DCs and $CD14^-CD68^-CD33^+$ immature myeloid cells (online supplemental table 2).

Imiquimod increased the numbers of epithelial $CD3^+CD8^-FOXP3^-$ T cells and stromal $CD14^+CD68^-CD11c^-$ monocytes, although this varied per patient. In addition, a steep decrease in macrophage counts, both stromal M1-like ($CD68^+CD163^-$) and epithelial and stromal M2-like ($CD68^+CD163^+$) macrophages, was observed in almost all patients on imiquimod treatment. The other major cell populations ($CD8^+$ T cells, $FOXP3^+$ regulatory T cells, $CD14^+$ monocytes, $CD11c^+$ DCs) did not overtly change on imiquimod treatment (figure 1C, online supplemental figure 2). Six months after imiquimod treatment, 21 patients had a complete response (CR), 3 patients a partial response (PR) and 11 patients were non-responders. To investigate whether the immunological response to imiquimod was different between CR and NR (PR not included in statistical analyses due to small sample size), the changes in composition of the immune microenvironment were studied (online supplemental figure 3A,B). During imiquimod treatment the median total intraepithelial T cell infiltrate was strongly increased in CR patients (p=0.015) (figure 2A). In particular, there was a higher influx of intraepithelial $CD3^+CD8^-FOXP3^-$ T cells and both stromal and intraepithelial $CD3^+CD8^-FOXP3^+$ regulatory T cells in CR patients but not in NR patients (online supplemental figure 3A). The number of intraepithelial and stromal $CD3^+CD8^-FOXP3^-$ T cells was much higher than their $FOXP3^+$ counterparts in these CR lesions (online supplemental table 2). The total number of infiltrating myeloid cells in the epithelium did not change much on imiquimod treatment in all patients (figure 2A). However, the stromal composition was changed in favor of $CD14^+$ myeloid cells (figure 2A), mainly because of a drastic decrease in classical ($CD68^+$) macrophages and $CD68^-CD14^-CD11c^+$ DCs (online supplemental figure 3B). Thus, successful lesion clearance on imiquimod treatment is associated with the potent accumulation of T cells. A depletion of macrophages was observed in the TME of all patients.

Quantitative and spatial pre-existing differences in lesion-infiltrating immune cells distinguish responders from non-responders

In order to develop a biomarker for response prediction, we focused on differences in the pre-existent intralesional immune infiltrate that were present before imiquimod treatment. The T cell and myeloid cell composition and absolute cell numbers were compared between CR vs NR in the pretreatment samples. The intraepithelial infiltrate was dominated by $CD3^+CD8^-FOXP3^-$ and $CD3^+CD8^+FOXP3^-$ T cells in CR patients, while $CD3^+CD8^-FOXP3^+$ regulatory T cells formed the largest fraction of T cells in NR patients (figure 2B). The epithelial region was mostly infiltrated by $CD14^+$ cells, however, this did not differ between the two patient groups (figure 2B). The fraction of stromal and intraepithelial M1-like macrophages was the largest in CR patients, whereas in NR patients these macrophages were mostly M2-like (figure 2B).

The number of total T cells did not differ between CR and NR, but clearly the total numbers of intraepithelial and stromal $CD3^+CD8^-FOXP3^-$ T cells were higher in CR patients, while the intraepithelial and stromal numbers of $CD3^+CD8^-FOXP3^+$ regulatory T cells were higher in NR patients (figure 2C, online supplemental figure 4A). The median myeloid cell counts were more than two-fold higher in CR compared with NR (figure 2A), with especially more intraepithelial and stromal presence of M1-like macrophages and $CD68^-CD14^-CD11c^+$ DCs in CR patients (figure 2C). Spearman correlation heatmaps revealed strong positive correlations between various stromal T cells and myeloid cells in CR, that were not found in NR (figure 2D).

An adequate antitumor response requires both sufficient numbers of infiltrating immune cells as well as a coordinated organization within the TME.[14] Using a multispectral imaging approach on FFPE tissue, we were able to investigate the *in situ* spatial interactions in cHSIL, and compared those between CR and NR. Clearly, T cells in CR and NR patients displayed different spatial interactions. In CR lesions different types of type 1 T cells were in close proximity ($CD3^+CD8^-FOXP3^-Tbet^+$ T cells with $CD8^+Tbet^+$ T cells). In contrast such type 1 T cells ($CD3^+CD8^-FOXP3^-Tbet^+$ T cells, $CD8^+Tbet^+$ T cells) were often directly spatially interacting with $CD3^+CD8^-FOXP3^+$ regulatory T cells in NR lesions (figure 3A). Notably, the regulatory T cells co-expressed Tbet, indicative for their specific capacity to suppress an ongoing type 1 T cell response.[15] Spatial myeloid cell interaction analysis revealed no distinct interaction pattern between CR and NR, indicating that especially the number and composition of the infiltrating myeloid cell pool rather than their interactions are associated with responsiveness. Altogether, these data suggest that a pre-existing coordinated strong infiltration with T cells and myeloid cells is required for adequate lesion clearance on imiquimod treatment.

Table 1 cHSIL imiquimod cohort patient characteristics

			Preimiquimod		10 weeks		20 weeks		6 months	
Patient ID	Age	Response	Histology	HPV PCR	Histology	HPV PCR	Histology	HPV PCR	Cytology	HPV PCR
ERAS 001	30	CR	CIN2	Positive	CIN1	Positive	No dysplasia	Negative	PAP1	x
MUMC 001	31	CR	CIN2-3	Positive	No dysplasia	Negative	No dysplasia	Negative	PAP1	x
MUMC 014	36	CR	CIN2	Positive	CIN1	Negative	No dysplasia	Negative	PAP1	Negative
MUMC 018	25	CR	CIN3	Positive	CIN2	Negative	No dysplasia	Negative	PAP1	x
MUMC 034	30	CR	CIN3	Positive	CIN1	Negative	No dysplasia	Negative	PAP1	Negative
MUMC 040	36	CR	CIN2	Positive	CIN1	Negative	No dysplasia	Negative	PAP1	Positive
MUMC 044	30	CR	CIN2	Positive	CIN1	Negative	No dysplasia	Negative	PAP1	Negative
MUMC 078	36	CR	CIN3	Positive	No dysplasia	Negative	No dysplasia	Negative	PAP1	x
MUMC 081	30	CR	CIN3	Positive	CIN2	Positive	No dysplasia	Negative	PAP1	Negative
MUMC 027	26	CR	CIN2	Positive	CIN1	Weak +	CIN1	Negative	PAP1	Positive
CATH 017	31	CR	CIN3	Positive	No dysplasia	Negative	CIN1	Negative	PAP1	x
ERAS 002	30	CR	CIN3	Positive	CIN1	Negative	CIN2	Negative	PAP1	x
ERAS 004	52	CR	CIN3	Positive	CIN1	Negative	CIN1	Negative	PAP1	x
ERAS 016	32	CR	CIN2	Positive	No dysplasia	Negative	CIN1	Positive	PAP1	Negative
MUMC 010	30	CR	CIN3	Positive	No dysplasia	Negative	CIN1	Positive	PAP1	Negative
MUMC 036	30	CR	CIN3	Positive	CIN3	Positive	CIN2	Negative	PAP1	x
MUMC 049	31	CR	CIN2	Positive	CIN1	Negative	CIN1	Negative	PAP1	Negative
MUMC 062	30	CR	CIN3	Positive	No dysplasia	Negative	CIN1	Negative	PAP1	Negative
MUMC 065	31	CR	CIN3	Positive	CIN1	Positive	CIN1	Negative	PAP1	x
CATH 006	30	CR	CIN3	Positive	CIN2-3	Positive	x	x	PAP1	Positive
MUMC 080	28	CR	CIN3	Positive	CIN1	Negative	CIN1	Negative	PAP1	Positive
CATH 023	30	PR	CIN3	Positive	CIN1	Negative	PAP2	Positive	PAP2	Positive
ERAS 006	33	PR	CIN2	Positive	x	Negative	CIN1	Positive	PAP3A2	Positive
MUMC 037	35	PR	CIN3	Positive	CIN1	Positive	CIN2	Negative	PAP2	x
CATH 012	29	NR	CIN2	Positive	No dysplasia	Negative	CIN3	Positive	x	x
ERAS 010	30	NR	CIN2	Positive	CIN1	Negative	CIN3	x	PAP4	Positive
MUMC 002	30	NR	CIN3	Positive	CIN2	Negative	CIN3	Positive	PAP2	Negative
MUMC 003	29	NR	CIN3	Positive	CIN3	Positive	x	x	PAP1	Negative
MUMC 008	30	NR	CIN3	Positive	CIN3	Positive	CIN3	Positive	PAP1	Negative
MUMC 024	31	NR	CIN3	Positive	CIN3	Positive	x	x	PAP1	Positive
MUMC 038	28	NR	CIN3	Positive	CIN3	Positive	CIN2	Positive	PAP1	Negative
MUMC 045	55	NR	CIN2	Positive	CIN1	Positive	CIN2	Positive	PAP3A1	Positive
MUMC 051	59	NR	CIN2	Positive	CIN3	Positive	x	x	PAP1	Negative
MUMC 064	36	NR	CIN3	Positive	CIN1	Negative	CIN3	Positive	PAP3A1	Positive
MUMC 079	36	NR	CIN3	Positive	CIN2	Weak +	CIN2	Positive	PAP1	x

cHSIL, cervical high-grade squamous intraepithelial lesion; CIN, cervical intraepithelial neoplasia; CR, complete response; NR, no response; PAP, Papanicolaou dysplasia classification for cervix smear cytology; PR, partial response; x, sample not available.

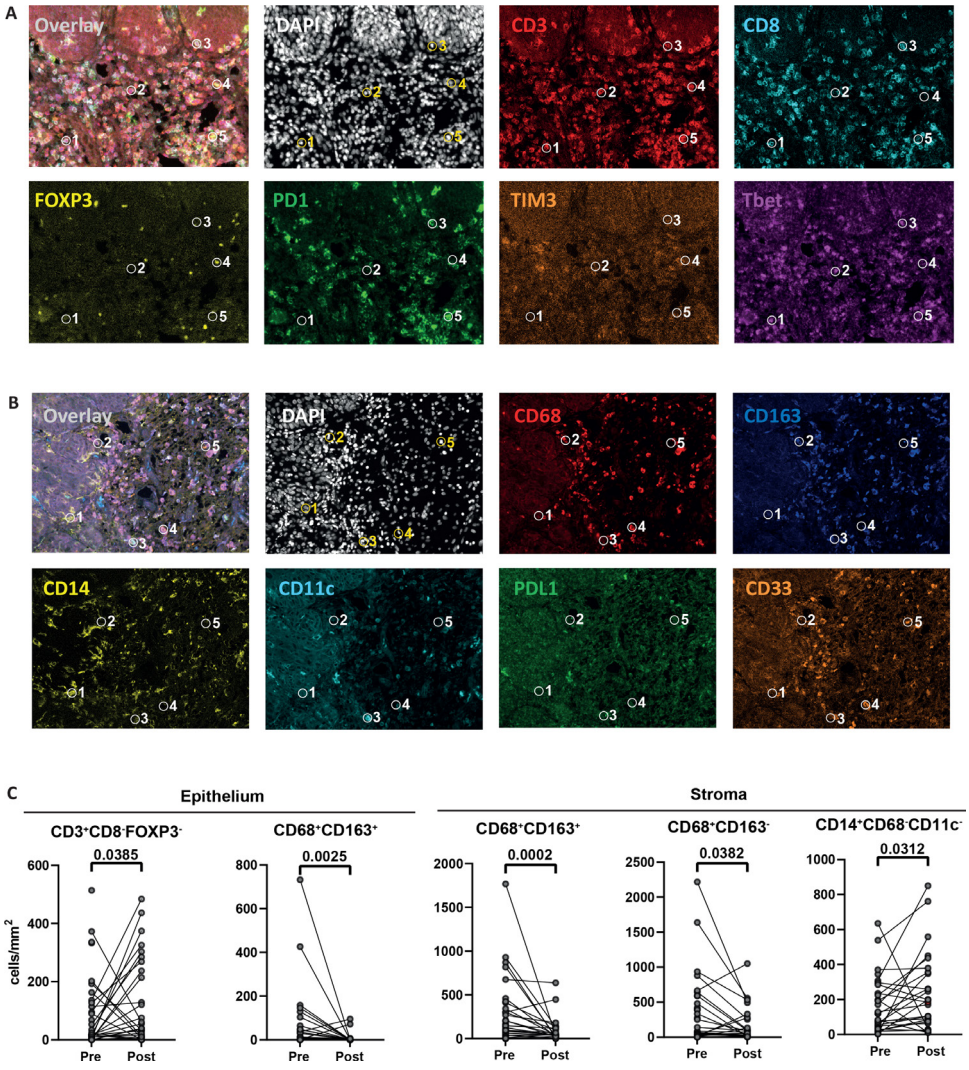

Figure 1 Multispectral imaging of cHSIL's immune tumor microenvironment pretreatment and on imiquimod treatment. (A) Multispectral immunofluorescence T cell panel, depicting the full seven color panel on a cHSIL biopsy, including all individual markers (DAPI, CD3, CD8, FOXP3, PD1, Tim3, Tbet). The full phenotypes of the encircled cells are: (1) $CD3^+CD8^+FOXP3^-Tbet^+$, 2) $CD3^+CD8^-FOXP3^-TBET^+$, (3) $CD3^+CD8^+FOXP3^-PD1^+Tbet^+$, (4) $CD3^+CD8^-FOXP3^+$ and (5) $CD3^+CD8^-FOXP3^-PD1^+$ (B) multispectral immunofluorescence myeloid cell panel, depicting the full seven color panel on a cHSIL biopsy, including all individual markers (DAPI, CD68, CD163, CD14, CD11c, PDL1, CD33). The full phenotypes of the encircled cells are: (1) $CD14^+CD68^-CD163^-$, (2) $CD14^-CD68^+CD163^+$, (3) $CD14^-CD68^-CD163^-CD11c^+$, (4) $CD14^-CD68^+CD163^-CD33^+$ and (5) $CD14^-CD68^-CD163^-CD33^+$. (C) Statistically significant changes (Wilcoxon paired signed rank test) in immune cell infiltration on imiquimod treatment in cHSIL's epithelium and stroma (n=35), as measured pretreatment and after 10 weeks of imiquimod treatment. cHSIL, cervical high-grade squamous intraepithelial lesion.

Immunohistochemical CIBI

The numbers of epithelium and stroma infiltrating $CD3^+CD8^-FOXP3^-$ T cells, M1-like macrophages and DCs were higher in CR, while the numbers of infiltrating $CD3^+CD8^-FOXP3^+$ regulatory T cells were lower compared with NR (figure 2C). This prompted us to examine if CR could be better distinguished from NR when these markers were combined into one quantitative biomarker. To this end, we created a combined biomarker, calculated as the sum of total $CD3^+CD8^-FOXP3^-$ T cells, total M1-like macrophages and total DCs, minus the total of $CD3^+CD8^-FOXP3^+$ regulatory T cells, either for the epithelium or for the stroma. Indeed, this biomarker clearly distinguished NR from CR (epithelium p=0.0001, stroma p<0.0001) (figure 4A,B).

Since the execution of an in-depth multispectral immunofluorescence analysis is not simple, hence not suitable to function as a widely implementable diagnostic biomarker, we explored whether a simplified biomarker could be developed that could be easily applicable in routine diagnostic pathology with a conventional light microscope. We, therefore, optimized a dual immunohistochemistry panel which allowed the separate identification of the immune markers positively (CD4, CD68, CD11c with DAB in brown) and negatively (FOXP3, CD163 with Vector Red in red) associated with clinical

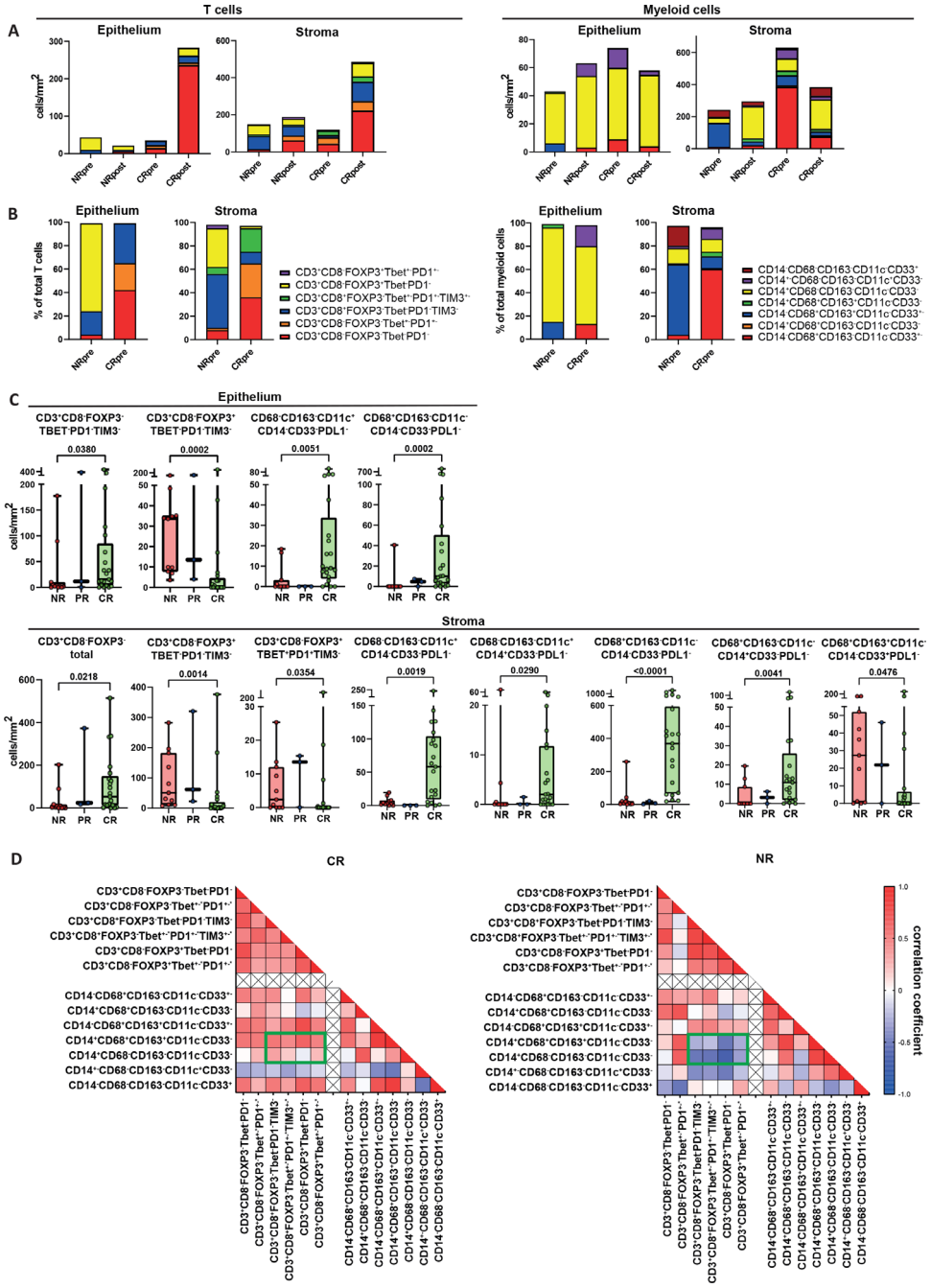

Figure 2 Pre-existing differences in immune cell composition between responders and non-responders to imiquimod. (A) Differences in median T cell and myeloid cell changes pretreatment and on imiquimod treatment in CR (n=21) and NR (n=11) cHSIL epithelium and stroma. In case of more than one marker indicated by +-, at least one of these markers is positive in that cell phenotype. (B) Pre-existing differences in composition of T cell and myeloid cell infiltrate in CR (n=21) vs NR (n=11) cHSIL epithelium and stroma. (C) Statistically significant differences (Mann-Whitney U test) in specific immune cell phenotypes infiltrating CR (n=21) vs NR (n=11) cHSIL epithelium and stroma. PR (n=3) not included in statistical analysis due to small sample size. (D) Spearman correlation heatmaps of pre-existing stromal T cell and myeloid cell infiltration, lineages separated by the crossed line, in CR (n=21) vs NR (n=11) cHSIL. The green square indicates the most striking differential correlations between CR versus NR. cHSIL, cervical high-grade squamous intraepithelial lesion; CR, complete responder; NR, non-responder; PR, partial response.

outcome in one tissue section (figure 5A, online supplemental table 1C). We validated the performance of this dual immunohistochemistry approach, by staining the entire cohort (n=35) and calculating the biomarker for both the epithelium and stroma. The overall cell counts in the dual immunohistochemistry biomarker were higher compared with the multispectral immunofluorescence biomarker. This was expected since immunohistochemistry strongly amplifies the signal of each detected marker, resulting in the detection of cells not only with a strong

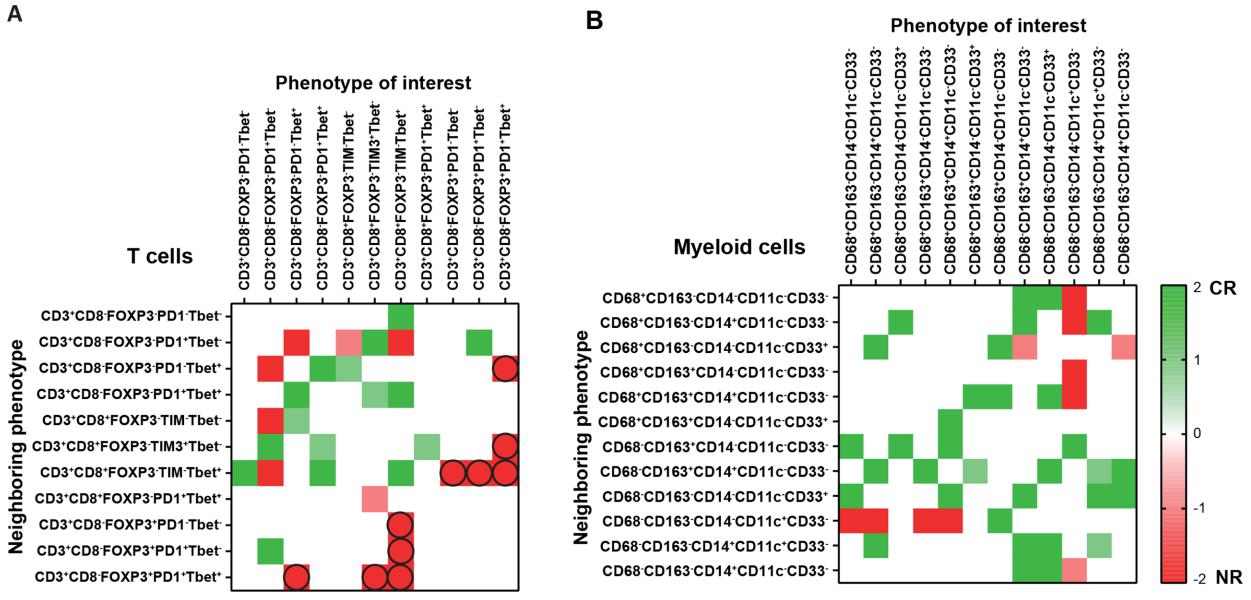

Figure 3 Differential spatial immune cell interactions in responders and non-responders to imiquimod. Heatmap of pre-existing differential spatial interactions between CR (n=21) and NR (n=11) cHSIL. A red interaction indicates that these two cell phenotypes frequently interact in NR lesions (more than expected based on chance, Z-score >2), and are spatially separated in CR lesions (Z-score <-2). A green interaction indicates that these two cell phenotypes frequently interact in CR lesions (more than expected based on chance, Z-score>2), and are spatially separated in NR lesions (Z-score<-2). (**A**) pre-existing differential T cell spatial interactions, and (**B**) pre-existing differential myeloid cell spatial interactions between CR and NR cHSIL. cHSIL, cervical high-grade squamous intraepithelial lesion; CR, complete responder; NR, non-responder.

but also with a weaker expression of the markers, whereas direct immunofluorescence only allows the detection of strongly positive cells. Despite the differences in detection method, the biomarker still excellently separated CR from NR, both in the epithelium (p<0.0001) (figure 5B) and in the stroma (p=0.0064) (figure 5C).

Given the clear demarcation of the epithelial compartment in cHSIL, allowing an easy and objective definition of the area in which the immune cells should be scored without interobserver variability, we analyzed the performance of the biomarker in the epithelium to distinguish CR from NR patients. The ROC curves for the epithelial biomarker calculated with the data of the multispectral immunofluorescence analysis (figure 6A) and of the dual immunohistochemistry analysis (figure 6B) were created. This showed excellent sensitivity and specificity of the predictive biomarker by both techniques, with an AUC of 0.89 (p=0.0003) by immunofluorescence, and an AUC of 0.95 (p<0.0001) by immunohistochemistry.

Since the numbers of intraepithelial FOXP3$^+$ and CD163$^+$ cells were relatively low when compared with their negative counterparts (online supplemental figure 5), we examined whether a further simplification of the dual immunohistochemical biomarker to a single color staining (DAB in brown, as conventionally used in pathology) could be achieved. For this we analyzed the performance of the biomarker without the detection of FOXP3 and CD163 by Vector Red, thus, only the detection of CD4, CD68 and CD11c by DAB. This simplification did not compromise the performance of the biomarker, as the sum of total intraepithelial CD4, CD68 and CD11c was well capable of distinguishing CR from NR patients (p<0.0001) (figure 6C), and the performance of this one color based biomarker still had an AUC of 0.95 (p<0.0001) (figure 6D). A threshold for this biomarker of intraepithelial CD4, CD68, CD11c cell counts >178.5 cells/mm2 provided the highest likelihood ratio (10.48), as well as sensitivity (95.24%) and specificity (81.82%) scores. In our cohort, this biomarker threshold accurately predicted complete response in 20/21 patients (positive

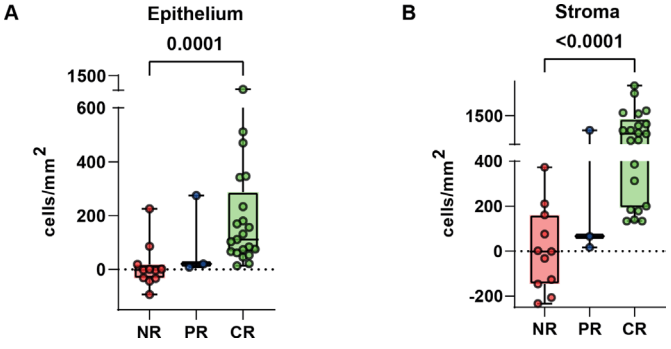

Figure 4 Multispectral immunofluorescence biomarker accurately distinguishes responders from non-responders (NRs). Multispectral immunofluorescence biomarker capability to distinguish CR (n=21) from NR (n=11) based on preimiquimod immunological cHSIL differences (Mann-Whitney U test), consisting of the sum of total CD3$^+$CD8$^-$ FOXP3$^-$ T cells, total CD68$^+$CD163$^-$ M1-like macrophages and total CD11c$^+$ dendritic cells, minus total CD3$^+$CD8$^-$ FOXP3$^+$ regulatory T cells, in (A) epithelium and (B) stroma. cHSIL, cervical high-grade squamous intraepithelial lesion; CR, complete responder.

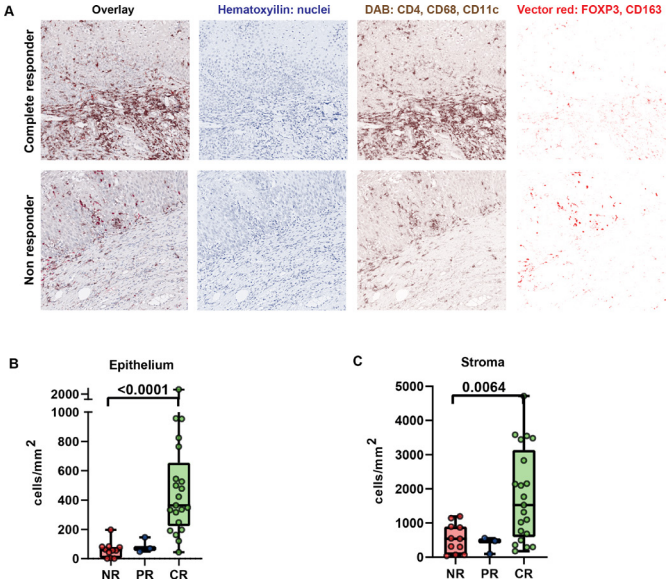

Figure 5 Dual immunohistochemical staining maintains accurate performance of predictive biomarker. (A) Overlay and individual colors of the dual immunohistochemistry panel staining on preimiquimod cHSIL of a CR and an NR patient, with the markers CD4, CD68 and CD11c visualized by DAB in brown, the markers FOXP3 and CD163 visualized by Vector Red in red, and hematoxylin as nuclear counterstain. (B) and (**C**) Immunohistochemical biomarker capability to distinguish CR (n=21) from NR (n=11) based on preimiquimod immunological cHSIL differences (Mann-Whitney U test). The biomarker was calculated as the sum of all cells with a completely brown membrane and unstained nucleus ($CD4^+$/$CD68^+$/$CD11c^+$ $FOXP3^-$ $CD163^-$) minus all cells with a brown membrane and red nucleus ($CD4^+$ $FOXP3^+$), for both the (B) epithelium and (C) stroma. cHSIL, cervical high-grade squamous intraepithelial lesion; CR, complete responder; NR, non-responder.

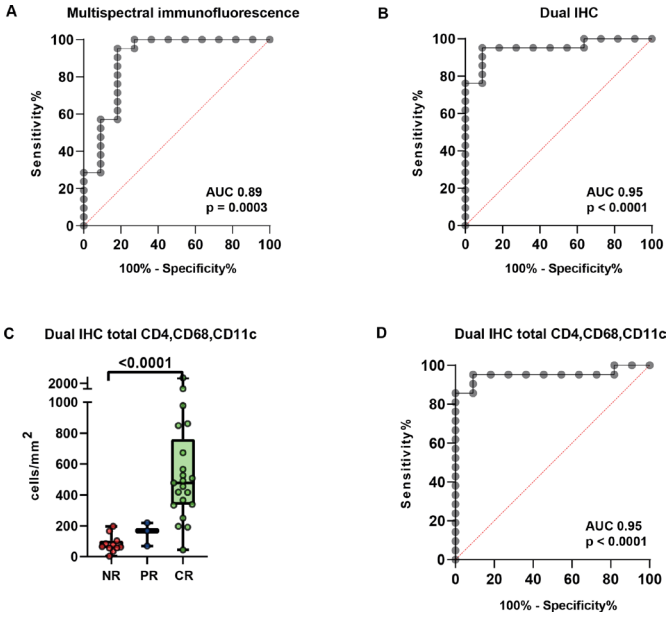

Figure 6 Simplified epithelial immune biomarker is excellent cHSIL immune biomarker for imiquimod (CIBI). (A) Multispectral immunofluorescence biomarker performance, consisting of the sum of total of $CD4^+$, $CD68^+CD163^-$ and $CD11c^+$ cells minus the total of $FOXP3^+$ cells in the epithelium as determined by the receiver operating characteristic (ROC) curve (n=32), and the same in (**B**) for the dual immunohistochemical biomarker. (C) Capability of the simplified epithelial dual immunohistochemistry biomarker, the sum of total $CD4^+$, $CD68^+$ and $CD11c^+$ cells, to distinguish CR (n=21) from NR (n=11) cHSIL (Mann-Whitney U test), and **(D)** its performance as determined by the ROC curve (n=32). cHSIL, cervical high-grade squamous intraepithelial lesion; CR, complete responder; NR, non-responder.

predictive value=95.24%), and no response in 10/11 patients (negative predictive value=90.91%). We designated this intraepithelial immune cell count biomarker the CHSIL Immune Biomarker for Imiquimod(CIBI).

DISCUSSION

This study is the first to identify a strong and easily applicable predictive biomarker for the clinical response of cHSIL patients to local immunotherapy with imiquimod, the CIBI. This biomarker is grounded on a comprehensive in-depth study of the phenotype and spatial composition of immune cells present in cHSIL, showing a strong relation between complete response to therapy and pre-existing $CD4^+$ T cell, M1-like macrophage and DC infiltration. These data formed the basis for a simple specific and sensitive single color immunohistochemical detection and scoring method with a positive and negative predictive value >90%, thereby adding significant value to the current <60% a priori chance of clinical response of cHSIL to imiquimod. The use of CIBI may be of great clinical value in the selection of patients responsive to imiquimod, hereby preventing unnecessary exposure to adverse effects of the intensive imiquimod treatment regimen. CIBI-based personalized therapy will improve therapy efficacy in the selected cHSIL patients, can be used to motivate therapy adherence, and may prevent surgical LLETZ treatment, thereby reducing the risk of potential future obstetric complications (ie, cervical insufficiency and subsequent premature deliveries).

The immune composition of cHSIL in patients with spontaneous regression includes all actors of the immune response required to mediate lesion clearance, and this can be observed in about 20% of cHSIL patients.[16 17] Spontaneous cHSIL regression is associated with a higher $CD8^+$ (granzyme B^+) and $CD4^+$ T cell infiltrate, and low infiltration by $CD25^+$ regulatory T cells and $CD138^+$ B cells, when compared with lesions that persisted.[16–20] Spontaneous cLSIL regression is associated with reduced $CD68^+$ macrophage infiltration compared with lesions that persisted.[21] In addition, high numbers of $CD4^+$ T cells, $Tbet^+$ T cells and $CD11c^+$ DCs are associated with the absence of recurrences after surgical therapy.[22] A bias inherent to this type of studies, is that about 20% of the CR patients could have had spontaneous lesion regression and display an immune cell composition, of which not all immune cell types are necessarily associated with

full regression after imiquimod treatment. To exclude the possibility that we would identify an immune cell composition associated with spontaneous regression rather than one associated with imiquimod-mediated regression, we focused only on those parameters that differed in the majority of CR patients when compared with NR patients. Interestingly, the pre-existing immune composition of patients with a spontaneous regression or an imiquimod-induced CR display a high level of similarity. Both contain relatively high numbers of $CD4^+$ T cells and DCs and low numbers of regulatory T cells.

Patients responding to imiquimod therapy displayed a steep on-treatment increase in infiltrating T cells, most likely activated ($PD1^+$) and/or with a type 1 cytokine profile ($Tbet^+$), after which the lesion was cleared. This suggests that the mechanism underlying the absence of spontaneous lesion regression is the lack of such T cell infiltration, which is rescued by imiquimod treatment. In addition, all patients treated with imiquimod displayed a decrease in macrophages, irrespective of their phenotype. One may speculate whether the decrease in M2-like macrophages is required in order for the T cells to infiltrate and execute an effective immune response as shown in other diseases.[23] However, imiquimod proved incapable of increasing the infiltration of T cells in NR patients, whose lesions displayed a strong pre-existing but not on-treatment M2-like macrophage infiltrate, precluding M2-like macrophages as a strong mediator of T cell suppression and suggesting that another mechanism prevents this. Potentially, regulatory T cells may have played a role in NR patients as in these lesions the regulatory T cells were not only abundantly present but also displayed direct spatial interactions with the other T cells, suggesting that they locally inhibited these T cells from executing their effector functions. The data of this study adds unique additional insight to our understanding of which immune cells are pivotal for cHSIL regression. Cell types that were present in low numbers in CR before treatment and did not increase on imiquimod treatment, that is, $CD8^+$ T cells, are not likely to form key mediators of lesion clearance. In addition, the cell types that are present in high numbers in both spontaneous and imiquimod-mediated complete regressions, and potentially increased by imiquimod, that is, $CD4^+$ T cells and $CD11c^+$ DCs, may causally be involved in cHSIL clearance.

HSIL lesions of the vulva also develop as a consequence of a persistent HPV infection and have been treated with imiquimod. Their immunological composition related to clinical outcome after imiquimod has been extensively studied. Our findings in cHSIL extend earlier observations in vHSIL, where imiquimod was found to increase the number of infiltrating $CD8^+$ T cells, $CD1a^+$ DCs and $CD94^+$ natural killer cells only in responders.[24] Both in cHSIL and vHSIL, a pre-existing coordinated high infiltration by pro-inflammatory T cells and myeloid cells is essential for response to imiquimod,[8] and a similar relation was found with response to therapeutic vaccination monotherapy in vHSIL.[9] There are some differences in the cell types associated with imiquimod response, which may reflect the two distinct anatomical sites.[25] In vHSIL, responders to imiquimod displayed a high infiltration with both $CD4^+$ T cells and $CD8^+$ T cells, whereas in cHSIL responders the $CD4^+$ T cells dominated. The correlation between a high infiltration of T cells and myeloid cells in responders suggests that cytokines produced by T cells (independent of being $CD4^+$ or $CD8^+$) play a role in this coordination.[10] Moreover, vHSIL responders already presented with high numbers of $CD14^+$ inflammatory myeloid cells, whereas in cHSIL mostly M1-like macrophages were present.[8] Altogether, these data in HSIL suggest that the foundation for the successful treatment of any HSIL by imiquimod, is the pre-existing abundant presence of T cells in combination with pro-inflammatory myeloid cells (either $CD14^+$ or M1-like). This fits well with preclinical data showing that the depletion or absence of these type of myeloid cells was associated with reduced lesion clearance.[26 27] Biologically this represents the onset of a coordinated antitumor immune response that is amplified by imiquimod and characterizes the HSIL responders.

There are two overt limitations to this study. First, the clinical response in this study was evaluated after biopsies and imiquimod treatment, so formally we cannot exclude that the clinical response observed is solely due to imiquimod treatment. Hence, CIBI might be a predictor for the clinical response after biopsy and imiquimod. However, since a biopsy is standard of care in the diagnostic work-up of cHSIL, this distinguishment is clinically irrelevant. Second, the number of patients currently analyzed was limited, precluding rigorous statistical compensation, hence our data should be viewed as hypothesis generating. Therefore, a new study (PRedICT-TOPIC, NCT05405270) is currently initiated to validate these findings prospectively in a large cohort and to test the implementation of CIBI in pathology laboratories.

In conclusion, the pre-existing difference in the total number of immune cell subsets found associated with imiquimod-induced regression of cHSIL can be exploited as accurate predictive biomarker in the clinic, based on the intraepithelial expression of CD4, CD68 and CD11c. We propose CIBI to be scored by publicly available open-source digital pathology image analyzers, so that it can be objectively implemented in the clinic.

Contributors Conceptualization: ZA, SHvdB, PJdVvS, EMGvE; Software: AS; Formal analysis: ZA; Resources: NH, AJK, AJMvdS, HJvB, JMJP, LK, BFMS, PJdVvS, EMGvE; Supervision: NFCCdM, SHvdB, PJdVvS, EMGvE; Funding acquisition: ZA, NFCCdM, SHvdB, EMGvE; Guarantor: SHvdB; Writing original draft: ZA, SHvdB, PJdVvS, EMGvE; Writing review and editing: ZA, NH, AJK, AS, AJMvdS, HJvB, JMJP, NFCCdM, LFSK, BFMS, SHvdB, PJdVvS, EMGvE.

Funding ZA received an MD/PhD grant from Leiden University Medical Center. NFCCdM received funding from the European Research Council under the European Union's Horizon 2020 research and innovation program (grant agreement number 852832). SHvdB received base funding from Oncode Institute. EMGvE received a clinical fellow grant from ZonMw.

Competing interests ZA, SHvdB, PJdVvS and EMGvE have filed for a patent on the CHSIL Immune Biomarker for Imiquimod (CIBI).

Patient consent for publication Consent obtained directly from patient(s)

Ethics approval Maastricht University Medical Center provided medical ethical approval for performing this study involving human particpants in the Netherlands, approval number: NL57849.068.16/METC162025. Participants gave informed consent to participate in the study before taking part.

Provenance and peer review Not commissioned; externally peer reviewed.

Data availability statement Data are available on reasonable request. All data relevant to the study are included in the article or uploaded as online supplemental information. All data generated during this study are included in this article and are available on reasonable request.

ORCID iDs
Ziena Abdulrahman http://orcid.org/0000-0001-9079-0293
Noel F C C de Miranda http://orcid.org/0000-0001-6122-1024
Sjoerd H van der Burg http://orcid.org/0000-0002-6556-0354

REFERENCES

1 Ting J, Rositch AF, Taylor SM, *et al*. Worldwide incidence of cervical lesions: a systematic review. *Epidemiol Infect* 2015;143:225–41.
2 van de Sande AJM, Schreuder CM, van Baars R, *et al*. Efficacy and long-term outcomes of repeated large loop excision of the transformation zone of the cervix. *Obstet Gynecol* 2022;139:417–22.
3 Abdulrahman Z, Kortekaas KE, De Vos Van Steenwijk PJ, *et al*. The immune microenvironment in vulvar (pre)cancer: review of literature and implications for immunotherapy. *Expert Opin Biol Ther* 2018;18:1223–33.
4 Fonseca BO, Possati-Resende JC, Salcedo MP, *et al*. Topical imiquimod for the treatment of high-grade squamous intraepithelial lesions of the cervix: a randomized controlled trial. *Obstet Gynecol* 2021;137:1043–53.
5 Grimm C, Polterauer S, Natter C, *et al*. Treatment of cervical intraepithelial neoplasia with topical imiquimod: a randomized controlled trial. *Obstet Gynecol* 2012;120:152–9.
6 Wouters T, Hendriks N, Koeneman M, *et al*. Systemic adverse events in imiquimod use for cervical intraepithelial neoplasia - A case series. *Case Rep Womens Health* 2019;21:e00105.
7 Hendriks N, Koeneman MM, van de Sande AJM, *et al*. Topical imiquimod treatment of high-grade cervical intraepithelial neoplasia (TOPIC-3): a nonrandomized multicenter study. *J Immunother* 2022;45:180–6.
8 Abdulrahman Z, de Miranda NFCC, Hellebrekers BWJ, *et al*. A pre-existing coordinated inflammatory microenvironment is associated with complete response of vulvar high-grade squamous intraepithelial lesions to different forms of immunotherapy. *Int J Cancer* 2020;147:2914–23.
9 Abdulrahman Z, de Miranda N, van Esch EMG, *et al*. Pre-existing inflammatory immune microenvironment predicts the clinical response of vulvar high-grade squamous intraepithelial lesions to therapeutic HPV16 vaccination. *J Immunother Cancer* 2020;8:e000563.
10 Abdulrahman Z, Santegoets SJ, Sturm G, *et al*. Tumor-specific T cells support chemokine-driven spatial organization of intratumoral immune microaggregates needed for long survival. *J Immunother Cancer* 2022;10:e004346.
11 Somarakis A, Van Unen V, Koning F, *et al*. ImaCytE: visual exploration of cellular Micro-Environments for imaging mass cytometry data. *IEEE Trans Vis Comput Graph* 2021;27:98–110.
12 Jackson HW, Fischer JR, Zanotelli VRT, *et al*. The single-cell pathology landscape of breast cancer. *Nature* 2020;578:615–20.
13 Ji AL, Rubin AJ, Thrane K, *et al*. Multimodal analysis of composition and spatial architecture in human squamous cell carcinoma. *Cell* 2020;182:1661–2.
14 Bindea G, Mlecnik B, Tosolini M, *et al*. Spatiotemporal dynamics of intratumoral immune cells reveal the immune landscape in human cancer. *Immunity* 2013;39:782–95.
15 Santegoets SJ, Duurland CL, Jordanova ES, *et al*. Tbet-positive regulatory T cells accumulate in oropharyngeal cancers with ongoing tumor-specific type 1 T cell responses. *J Immunother Cancer* 2019;7:14.
16 Ovestad IT, Gudlaugsson E, Skaland I, *et al*. The impact of epithelial biomarkers, local immune response and human papillomavirus genotype in the regression of cervical intraepithelial neoplasia grades 2-3. *J Clin Pathol* 2011;64:303–7.
17 Munk AC, Gudlaugsson E, Ovestad IT, *et al*. Interaction of epithelial biomarkers, local immune response and condom use in cervical intraepithelial neoplasia 2-3 regression. *Gynecol Oncol* 2012;127:489–94.
18 Kojima S, Kawana K, Tomio K, *et al*. The prevalence of cervical regulatory T cells in HPV-related cervical intraepithelial neoplasia (CIN) correlates inversely with spontaneous regression of CIN. *Am J Reprod Immunol* 2013;69:134–41.
19 Trimble CL, Clark RA, Thoburn C, *et al*. Human papillomavirus 16-associated cervical intraepithelial neoplasia in humans excludes CD8 T cells from dysplastic epithelium. *J Immunol* 2010;185:7107–14.
20 Woo YL, Sterling J, Damay I, *et al*. Characterising the local immune responses in cervical intraepithelial neoplasia: a cross-sectional and longitudinal analysis. *BJOG* 2008;115:1616–22. discussion 21-2.
21 Hammes LS, Tekmal RR, Naud P, *et al*. Macrophages, inflammation and risk of cervical intraepithelial neoplasia (CIN) progression--clinicopathological correlation. *Gynecol Oncol* 2007;105:157–65.
22 Origoni M, Parma M, Dell'Antonio G, *et al*. Prognostic significance of immunohistochemical phenotypes in patients treated for high-grade cervical intraepithelial neoplasia. *Biomed Res Int* 2013;2013:1–7.
23 Peranzoni E, Lemoine J, Vimeux L, *et al*. Macrophages impede CD8 T cells from reaching tumor cells and limit the efficacy of anti-PD-1 treatment. *Proc Natl Acad Sci U S A* 2018;115:E4041–50.
24 van Seters M, van Beurden M, ten Kate FJW, *et al*. Treatment of vulvar intraepithelial neoplasia with topical imiquimod. *N Engl J Med* 2008;358:1465–73.
25 Santegoets SJ, van Ham VJ, Ehsan I, *et al*. The anatomical location shapes the immune infiltrate in tumors of same etiology and affects survival. *Clin Cancer Res* 2019;25:240–52.
26 Beyranvand Nejad E, Labrie C, Abdulrahman Z, *et al*. Lack of myeloid cell infiltration as an acquired resistance strategy to immunotherapy. *J Immunother Cancer* 2020;8:e001326.
27 van der Sluis TC, Sluijter M, van Duikeren S, *et al*. Therapeutic peptide vaccine-induced CD8 T cells strongly modulate intratumoral macrophages required for tumor regression. *Cancer Immunol Res* 2015;3:1042–51.